Journal of Cellular Biochemistry 92:238–248 (2004)

Expression of Nox4 in Osteoclasts

Su Yang,* Yizhong Zhang, William Ries, and Lyndon Key

Department of Pediatrics, Medical University of South Carolina, Charleston, SC 29425

Abstract A new superoxide-generating enzyme, NADPH oxidase 4 (Nox4), contributes to osteoclastic superoxide production. In this study, we demonstrated that Nox4 is expressed at a higher level in osteoclasts than that in precursor cells. This result suggested that Nox4 is upregulated during the differentiation and development of osteoclasts. Cotransfection of Nox4/P22 DNA resulted in enhanced superoxide production in osteoclasts, indicating that P22 may be a necessary factor for the Nox4 activity. In addition, expression of both cathepsin K and TRAP is increased significantly in osteoclasts cotransfected with Nox4/P22. Further study revealed that JNK was activated and that NF-κB was inhibited in Nox4/P22 cotransfected osteoclasts. These findings suggest that superoxide and/or superoxide derived molecules may modulate the signal transduction pathways necessary for osteoclasts to function. J. Cell. Biochem. 92: 238–248, 2004.

Key words: NADPH oxidase; Nox; superoxide; osteoclast

Garrett et al. [1990] and Key et al. [1990] demonstrated that superoxide was generated by osteoclasts and was related to their bone resorptive activity. Since superoxide is generated on the external membrane of the osteoclast and is located at the ruffle-border area [Key et al., 1990], there is consistency with the concept that superoxide contributes to bone resorption. A superoxide scavenger, the desferal-manganese complex (DMnC), reduced the amount of osteoclastic superoxide, and resulted in a decrease of bone resorption in a dose-dependent manner [Ries et al., 1992]. Key et al. [1994] demonstrated that osteocalcin, one of the noncollagenous bone matrix proteins, was fragmented into small peptides upon exposure to superoxide. Superoxide was produced by osteoclasts in an extracellular compartment and even in the absence of other enzymes, superoxide was capable of degrading bone matrix proteins. The destructive properties of superoxide (and possibly other oxygen radicals) contribute to degradation of matrix proteins, making them more susceptible to enzyme digestion [Hall et al., 1995]. Evidence suggests that, in the absence of superoxide, acidification of the ruffled border, and removal of bone minerals continue, but matrix fibrils are left behind because the bone matrix is not completely degraded [Ries et al., 1992]. In addition, Garrett et al. [1990] found that superoxide stimulates the formation of osteoclasts. Thus, superoxide appears to be directly involved in bone degradation and in osteoclast formation.

NADPH oxidase has been shown to be an enzyme system generating superoxide in osteoclasts [Steinbeck et al., 1994; Yang et al., 1998]. A rate-limit subunit of NADPH oxidase is p91. Osteoclasts from p91 knockout mice continued to produce superoxide at a normal rate. This unexpected phenomenon led us to clone mouse NADPH oxidase 4 (Nox4), a new homologue of p91 [Yang et al., 2001]. Abrogation of the normal level of Nox4 expression in osteoclasts inhibits both osteoclastic superoxide production and bone resorption activity [Yang et al., 2001].

Production of superoxide is an important aspect of osteoclast-mediated bone resorption. Studies have shown that an increase or decrease of superoxide production has been associated with stimulated or inhibited osteoclastic bone resorption [Ries et al., 1992; Berger et al., 2001]. To generate a highly active osteoclast model in vitro, we attempted to mimic the high production of superoxide in osteoclasts by the DNA transfection technology. In this study, a gain of function strategy using the DNA

Grant sponsor: SC the Commission on Higher Education (to SY); Grant number: R00-M23.

*Correspondence to: Su Yang, CSB 316, MUSC, Charleston, SC 29425. E-mail: yangs@musc.edu

Received 5 September 2003; Accepted 29 December 2003

DOI 10.1002/jcb.20048

transfection technique is applied. This technique examines the hypothesis that Nox4-derived superoxide production may be involved in osteoclast formation and that expression of Nox4 may enhance osteoclast activity.

We expect that not only is Nox4 involved in bone resorption, but that it also functions in regulating the osteoclast signaling pathway by generating superoxide and/or other reactive oxygen species (ROS). We have shown here that increased superoxide generation by Nox4/P22 transfection related with a greater expression of cathepsin K and TRAP in RAW derived osteoclasts. JNK was activated and NF-κB was inhibited in Nox4/P22 cotransfected osteoclasts. These findings suggest that superoxide and/or superoxide derived molecules may modulate the signal transduction pathways necessary for osteoclasts to function.

MATERIALS AND METHODS

Materials

Recombinant murine RANKL is a gift from Amgen, Inc. (Thousand Oaks, CA). M-CSF, and other chemical reagents were purchased from Sigma (St. Louis, MO). IQ SYBR Green Supermix for a real-time PCR was obtained from Bio-Rad (Hercules, CA). The anti-JNK antibody was purchased from Santa Cruz (Santa Cruz, CA). SuperFect reagent was bought from Qiagen (Valencia, CA), and expression vector pcDNA3.1/V5-his was purchased from Invitrogen. The in situ hybridization (ISH) system for use with biotinylated probes was purchased from DAKO (Carpinteria, CA). The reagent for measuring TRAP (Tartrate resistant acid phosphatases) activity was purchased from RAICHEM (San Diego, CA).

RAW Derived Osteoclasts

Mouse macrophage cell line RAW 264.7 differentiated into fully functional osteoclasts in the presence of RANKL [Hsu et al., 1999]. RAW 264.7 cells were cultured in DMEM/10% FBS containing 50–100 ng/ml RANKL. RAW derived osteoclasts were formed after 5–7 days, and 80% of the cell population appeared to be osteoclasts that were identified as TRAP positive cells with more than three nuclei.

Bone Marrow Derived Osteoclasts

Osteoclasts obtained from mouse bone marrow cells were prepared as described [Wei et al., 2002]. Briefly, bone marrow cells from 4–6-week-old mice were cultured at 65,000/cm^2 in α-MEM/10% FBS with 10 ng/ml M-CSF for 24 h. The non-adherent cells were harvested and transferred to a new dish. RANKL then was added to dishes (f.c. 100 ng/ml). The medium was changed every three days by adding 5 ml of α-MEM/10% FBS with 10 ng/ml M-CSF and 100 ng/ml RANKL, replacing the old medium. Osteoclasts were observed as giant osteoclasts having three or more nuclei after culture for 7–10 days. Non-osteoclast cells were treated by a brief enzyme digestion (10 min with pronase-EDTA solution) and removed by gentle pipetting. More than 80% of the remaining cells were TRAP positive osteoclasts.

In Situ Hybridization

Plasmid DNA containing the reverse orientation of Nox4 was linearized by Not I, and biotin labeled Nox4 antisense RNA was generated by T7 RNA polymerase. To produce a smaller size of riboprobes, alkaline hydrolysis was conducted at 60°C for 30 min in a solution of 60 mM Na_2CO_3; 40 mM $NaHCO_3$, pH 10.2. The size of the riboprobes (100–300 base) was verified by electrophoresis.

Murine paws were dissected from newborn mice and cryosections were cut. After fixing in buffered 10% formalin, slides were rinsed three-times in TBS (50 mM Tris-Cl, pH 7.6, 0.15 M NaCl). Meanwhile, riboprobes were diluted to 0.2–1 μg/ml using a hybrid solution (DAKO, S3304), and denatured at 80°C for 10 min. One drop of the diluted riboprobe solution was applied to each section, and a coverslip was placed. Slides then were placed in a humid box with wet paper towels, and hybridization was conducted at 37°C overnight. At the end of hybridization, slides were immersed in a TBS bath until the coverslips came off. Slides were washed with a pre-warmed 40°C wash solution and incubated at 40°C for 30 min. Thereafter, slides were washed 2× in a fresh TBS for 1 min. Streptavidine-AP reagent was applied and incubated for 20 min at RT. Finally, slides were washed in a fresh TBS for 5 min and air dried.

For ISH using cultured osteoclasts, murine bone marrow cells were cultured in chamber slides in the presence of M-CSF and RANKL to obtain osteoclasts. After fixing, slides were treated with 0.1% Triton for 5 min to increase cell permeability. ISH was performed as described above.

Expression Vector and Transient Transfection

Full-length cDNA of Nox4 [Yang et al., 2001] was subcloned into the pcDNA3.1/V5-his vector. Mouse P22 cDNA was generated by RT-PCR based on the GenBank information (gi: 22094076). It was subsequently subcloned into the pcDNA3.1/V5-his vector.

When RAW derived osteoclasts were formed in culture, transient transfection was conducted according to the manufacture's manual. Briefly, 5 μg of DNA was diluted in 150 μl of the culture medium containing no serum or antibiotics. Thirty microliters of SuperFect reagent then was added to the DNA solution, and incubated at RT for 5–10 min to allow formation of the transfection DNA complex. After the incubation, 1 ml of culture medium containing serum and antibiotics was added to the DNA tube. Thereafter, culture dishes were washed once with 5 ml of PBS, and the mixture of the transfection DNA complex (1,180 μl) was immediately transferred to the culture dish. Cells were incubated with the transfection complex at 37°C, 5% CO_2 for 2–3 h. After removing the medium containing the transfection complex by gentle aspiration, cells were washed once with PBS. Fresh medium containing 50 ng/ml of RANKL then was added and incubation was conducted for 1–2 days. The cell viability after transfection was approximately 90%. Successful transfection was demonstrated by overexpression of Nox4 mRNA identified by the real-time PCR (Table II).

Superoxide Production Assay

RAW derived osteoclasts were transfected and cultured for 24 h as described above. Superoxide production was measured by a NBT assay [Key et al., 1990]. Briefly, RAW derived osteoclasts were incubated with the NBT solution (2 mg/ml NBT and 35% FBS in culture medium) for 1 h at 37°C. Thereafter, cells were fixed by 10% formalin. The NBT staining intensity of one individual osteoclast was measured and quantified by an inverted microscope equipped with a CCD camera, and the C2D densitometry software. Twenty NBT-stained RAW derived osteoclasts from each experiment were randomly selected and analyzed.

RT-PCR and Real-Time PCR

Total RNA was extracted using RNAzol reagent, and 2 μg of RNA was converted to cDNA by reverse transcription. Conventional PCR was performed using 3–5 μl of cDNA mixture and PCR primers as indicated (Table I). Real-time PCR then was conduced by the iCycler iQ real-time PCR detection system (Bio-Rad) using 0.1–1 μl cDNA mixture and PCR primers as indicated (Table I). A standard curve with known copy numbers of 18S rRNA was generated by serial dilutions and used for each run. Amplification of 18S rRNA from the same sample was used as the internal standard, and its copy number was determined according to the standard curve. A relative expression level of target mRNA was expressed as copy numbers per 10^7 copies of 18S rRNA.

TRAP Activity

RAW derived osteoclasts were transfected and cultured for 24 h as described above. After washing by PBS, cells were lysed in RIPA buffer and protein concentration was determined by

TABLE I. PCR Primers

Mouse gene	Primer sequence (5′–3′)	Position	Accession number
Primers for real-time PCR			
Nox4	Forward: CCCAAGTTCCAAGCTCATTTCC	5′: 868	AF218723
	Reverse: TGGTGACAGGTTTGTTGCTCCT	3′: 958	
Cathepsin K	Forward: GTGGTTCCTGTTGGGCTTTCA	5′: 407	XM_109390
	Reverse: CCGCCTCCACAGCCATA	3′: 523	
TRAP	Forward: GTCCATCGCCGAGCAC	5′: 765	NM_007388
	Reverse: AGCCCACACCGTTCTCGTCCT	3′: 881	
c-fms	Forward: GGTTGTAGAGCCGGGTGAAAC	5′: 165	X68932
	Reverse: CTTCCGGGAGATTCAGGGTC	3′: 256	
18S RNA	Forward: GGGATGCGTGCATTTATCAGA	5′: 208	22550391
	Reverse: GTCACCCGTGGTCACCAT	3′: 394	
Primers for conventional PCR			
GAPDH	Forward: GGTCACCAGGGCTGCCATTTG	5′: 91	M32599
	Reverse: ATTGCTGACAATCTTGAGTGA	3′: 467	
Nox4	Forward: CAGCTTCTACCTACGCAATA	5′: 575	AF218723
	Reverse: GGAAATGAGCTTGGAACTTGGG	3′: 868	
	Probe for hybridization: AATGTAGACACTCACCCTCCT	5′: 700	

the protein assay reagent (Bio-Rad). Cell lysates samples (0.05 ml) were mixed with acid phosphatases reagent (1 ml) and tartrate solution (0.01 ml). After incubation for 5 min at 30°C, the initial absorbance at 405 nm was read. Final absorbance was read after samples continued to incubate for 5 min at 30°C. TRAP activity (U/L) was calculated by $\Delta A/\text{min} \times (1.06 \times 10^6/12.9 \times 10^3/0.05)$ as suggested by the manufacturer. Finally, TRAP activity (U/L) was converted to U/mg protein.

EMSA

Nuclear proteins were extracted as described with a slight modification [Andrews and Faller, 1991]. EMSA was performed by a modification of a method previously described [Singh et al., 1986]. Briefly, 10 μg of nuclear proteins were suspended in 20 μl of binding buffer (12 mM HEPES-K, pH 8, 4 mM Tris-Cl, pH 8, 60 mM KCl, 30 mM NaCl, 5 mM MgCl, 0.1 mM EDTA, 0.1 mg/ml BSA, 12.5% glycerol, 1 mM DTT, 50 μg/ml Poly(d[I-C]), 0.5 mM PMSF, 50,000 cpm of the ^{32}P-labeled NF-κB consensus sequence (5′-AGCTTGGGGACTTTCCGAG-3′) with or without 50 ng of unlabeled oligonucleotide. After incubation at room temperature for 30 min, the DNA–protein complexes were resolved by electrophoresis on 4% polyacrylamide gel. The autoradiography was processed to reveal the binding activity of the DNA–protein complexes.

Kinase Assay

RAW derived osteoclasts were transfected and cultured for 24 h as described above. After washing by PBS, osteoclasts were lysed by adding 1 ml of RIPA buffer and incubated for 30 min at 4°C. After centrifugation, the supernatant containing total cell extracts was precleared with 10–15 μl of protein A/G-agarose beads. The beads then were removed by centrifugation and the supernatant (500 μg) was incubated with 1 μg of anti-JNK antibody (Santa Cruz) for 2–3 h at 4°C. The JNK immunocomplexes were precipitated by protein A/G-agarose beads. After several washings, the beads were resuspended in 25 μl of kinase buffer containing 25 μM of ATP, 2 μCi of [γ-^{32}P] ATP, and 1 μg of recombinant c-Jun protein as a substrate. Incubation was conducted at 30°C for 30 min, and 30 μl of 2× sample buffer then was added. After boiling for 5 min, samples were separated by 12% SDS–PAGE, and followed by autoradiography to determine the ^{32}P-labeled c-Jun protein at a position of 37 kDa.

Statistical Analysis

Results were expressed as mean ± SD. Differences between means were determined by the Student's *t*-test.

RESULTS

Expression of Nox4 in Osteoclasts

Expression of Nox4 in osteoclasts was demonstrated by ISH. Figure 1A shows hybridization signals located at the collar region in the newborn murine paw, where osteoclastic activity initiates vascularization of the cartilaginous bone model or anlage. Figure 1B shows that multinuclear cells are heavily stained while mononuclear cells are stained very lightly, indicating Nox4 expression in osteoclasts. To confirm this result, a conventional RT-PCR was performed. As shown in Figure 1C, Nox4 mRNA was expressed in osteoclasts while the precursor cells (RAW and bone marrow) had an infinitesimal amount of Nox4 mRNA. Our data showed that as osteoclasts developed from precursor cells, expression of Nox4 was increased. Upregulation of Nox4 suggests that Nox4 may be of physiological importance in the development and formation of osteoclasts.

Nox4 Transfection of RAW Derived Osteoclasts

To generate a highly active osteoclast model in vitro, we attempted to mimic the high production of superoxide in osteoclasts by the DNA transfection technology. An in vitro expression system was constructed by inserting the Nox4 cDNA coding sequence into an expression vector, driven by a CMV promoter (pcDNA3.1/V5-his, Invitrogen). RAW-derived osteoclasts were transfected with Nox4, a control DNA, P22, R-Nox4/P22, and Nox4/P22, respectively. After culturing for 24 h in the presence of RANKL, RNA was isolated for RT-PCR. The high expression of Nox4 mRNA in transfected osteoclasts was demonstrated by a real-time PCR (Table II).

Osteoclastic superoxide production activity was determined by the NBT assay. Figure 2 showed that cotransfection of Nox4 with P22 greatly enhanced osteoclastic superoxide production. This finding suggests that Nox4 may require an accessory protein P22 to produce superoxide in a manner similar to the P91 subunit. When superoxide dismutase (SOD) was

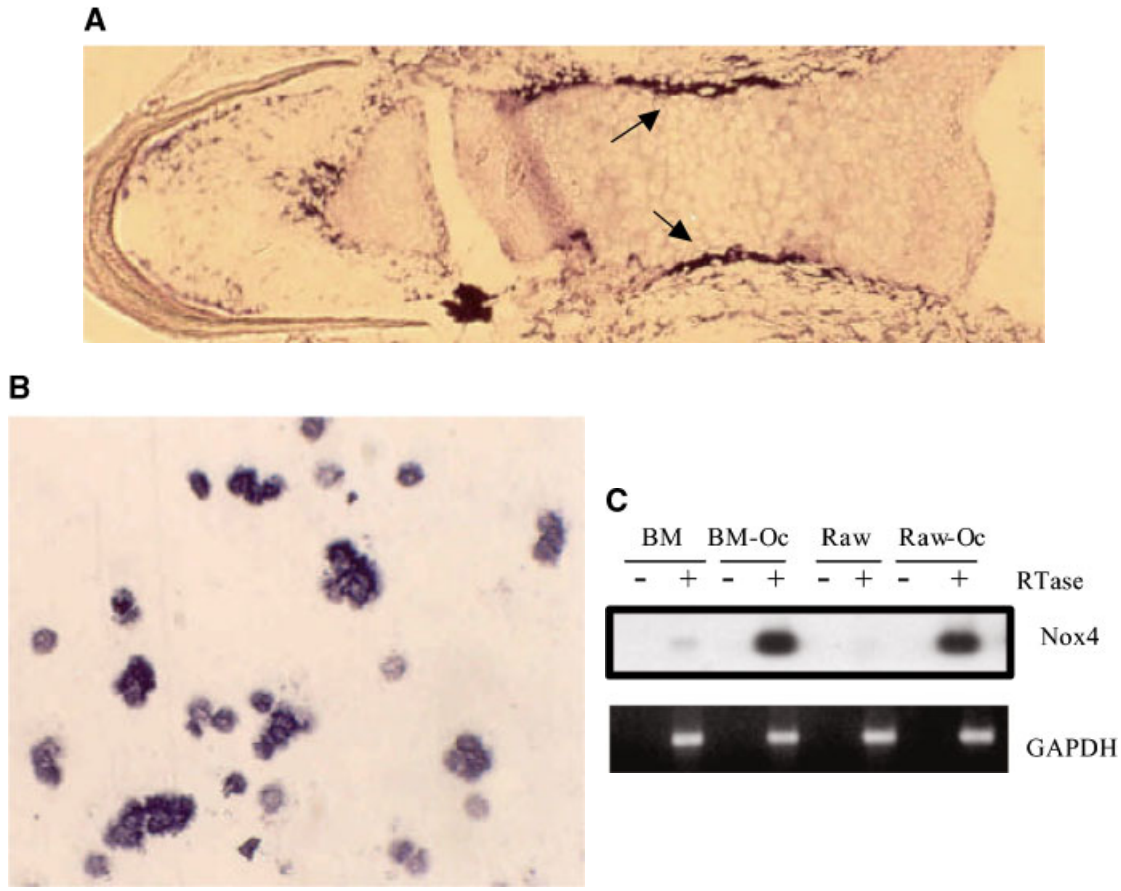

Fig. 1. NADPH oxidase 4 (Nox4) expression in osteoclasts. **A**: Murine paws were dissected from newborn mice and cryosections were cut. After fixing, biotin labeled Nox4 antisense RNA was applied to the slides, and ISH was conducted at 37°C overnight in a humid box, as described in Materials and Methods. Arrows indicate the intensive signals are located at the collar region in the newborn murine paw where osteoclastic activity initiates vascularization of the cartilaginous bone model. **B**: Murine bone marrow cells were cultured in chamber slides in the presence of M-CSF and RANKL to obtain osteoclasts. After fixing, slides were treated with 0.1% Triton for 5 min to increase cellular permeability. ISH was performed as described in Materials and Methods. Note that multinuclear cells are heavily stained while some mononuclear cells are stained very lightly, indicating Nox4 expression in osteoclasts. **C**: RNA was isolated from osteoclasts originated from mouse bone marrow and RAW cells, respectively. RT-PCR was performed using Nox4 primers (Table I). The specificity of the PCR product was demonstrated by the Southern blot using a ^{32}P-labeled internal probe. The presence of Nox4 is shown in osteoclasts, but not in precursor cells (BM and RAW). PCR amplifications of GAPDH were served as positive controls, and negative controls were the same samples to which RTase was not added. Shown here is one of three repeat experiments. RTase: reverse transcriptase. BM, bone marrow; Oc, osteoclasts. [Color figure can be viewed in the online issue, which is available at www.interscience.wiley.com.]

TABLE II. Expression of Nox4 mRNA in Transfected Osteoclasts

	Nox4
Control vector	$0.8 \times 10^4 \pm 1.5 \times 10^3$
Nox4	$76.0 \times 10^4 \pm 8.3 \times 10^3$*
P22	$6.4 \times 10^4 \pm 2.1 \times 10^3$
R-Nox4/P22	$15.1 \times 10^4 \pm 5.7 \times 10^3$
Nox4/P22	$96.0 \times 10^4 \pm 8.9 \times 10^3$*

RAW-derived osteoclasts were transfected with a control vector, Nox4, P22, R-Nox4/P22, and Nox4/P22 DNAs, respectively. Expression of Nox4 mRNA in transfected osteoclasts was analyzed by a real-time PCR as described in the methodology. Results were expressed as mean ± SD of mRNA copy number per 10^7 copies of 18S rRNA.
R-Nox4, the reverse orientation of Nox4.
*$P < 0.01$.

included in the assay, no superoxide was detectable (data not shown), suggesting the specificity of the superoxide generated by transfected cells. Increased superoxide production was abolished when cells were cotransfected with P22/R-Nox4 (the reverse orientation of Nox4), indicating that enhanced superoxide production might be linked to an increase of Nox4 expression in transfected RAW derived osteoclasts.

Expression of Cathepsin K and TRAP in Transfected Cells

To show whether a Nox4 DNA transfection could affect osteoclastic gene expression, a

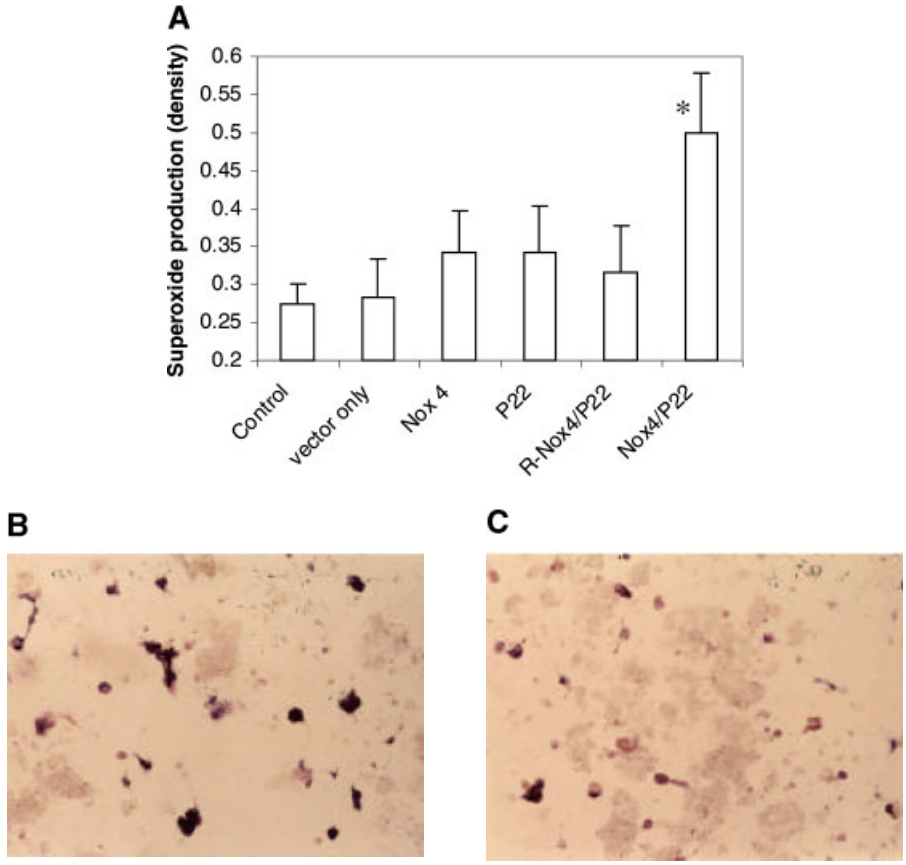

Fig. 2. Superoxide production by transfected osteoclasts. **A**: RAW-derived osteoclasts were transfected with a control vector, Nox4, P22, R-Nox4/P22, and Nox4/P22 DNAs, respectively. After culturing for 24 h, the superoxide generating activity of transfected osteoclasts was determined by the NBT assay and quantified using a CCD camera equipped with the C2D densitometry software. Data were collected from 20 randomly selected osteoclasts in each experiment. The maximum of superoxide generation was observed in osteoclasts transfected with Nox4/P22. R-Nox4, the reverse orientation of Nox4. Results were expressed as mean ± SD. $^*P < 0.05$. **B**: NBT stained osteoclasts transfected with Nox4 and p22. **C**: NBT stained osteoclasts transfected with a control DNA. [Color figure can be viewed in the online issue, which is available at www.interscience.wiley.com.]

real-time PCR was performed. Table III showed that mRNA expression of cathepsin K and TRAP was increased in osteoclasts cotransfected with Nox4/p22 DNAs, while no significant increase of c-fms (M-CSF receptors) was observed. In addition, enhanced TRAP activity was observed in osteoclasts cotransfected with Nox4/p22 DNAs (Fig. 3).

Notably, when cells were transfected with the reverse oriented Nox4 (R-Nox4), both cathepsin K and TRAP expression levels were declined, which may indicate a decreased osteoclastic

TABLE III. Expression of Cathepsin K, TRAP, and c-fms in Transfected Osteoclasts

	Cathepsin K	TRAP	c-fms
Control vector	$5.8 \times 10^4 \pm 1.5 \times 10^3$	$4.8 \times 10^4 \pm 1.1 \times 10^3$	$5.2 \times 10^4 \pm 3.3 \times 10^3$
Nox4	$5.0 \times 10^4 \pm 4.3 \times 10^3$	$4.5 \times 10^4 \pm 4.7 \times 10^3$	$3.9 \times 10^4 \pm 4.3 \times 10^3$
P22	$4.3 \times 10^4 \pm 6.1 \times 10^3$	$4.4 \times 10^4 \pm 2.1 \times 10^3$	$3.1 \times 10^4 \pm 0.7 \times 10^3$
R-Nox4/P22	$2.1 \times 10^4 \pm 0.7 \times 10^3$	$1.6 \times 10^4 \pm 4.9 \times 10^3$	$2.3 \times 10^4 \pm 3.2 \times 10^3$
Nox4/P22	$12.0 \times 10^4 \pm 0.9 \times 10^3$*	$17.0 \times 10^4 \pm 16 \times 10^3$*	$4.7 \times 10^4 \pm 3.6 \times 10^3$

RAW-derived osteoclasts were transfected with a control vector, Nox4, P22, R-Nox4/P22, and Nox4/P22 DNAs, respectively. Expression of cathepsin K, TRAP, and c-fms in transfected osteoclasts were analyzed by a real-time PCR as described in the methodology. Results were expressed as mean ± SD of mRNA copy number per 10^7 copies of 18S rRNA.
R-Nox4, the reverse orientation of Nox4.
$^*P < 0.05$.

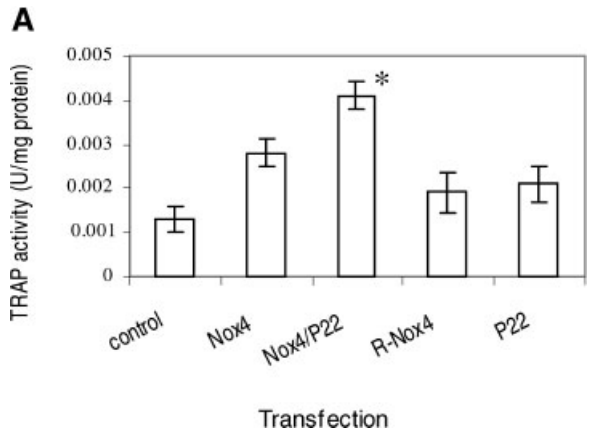

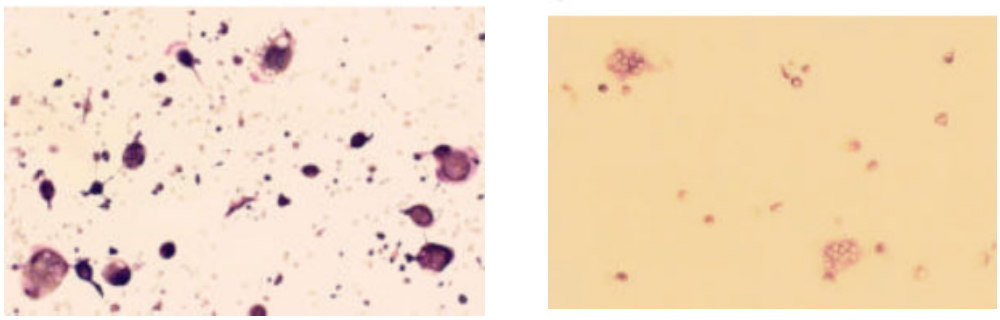

Fig. 3. TRAP activity in transfected osteoclasts. **A**: RAW-derived osteoclasts were transfected with a control vector, Nox4, R-Nox4/P22, and Nox4/P22 DNAs, respectively. After culturing for 24 h, osteoclasts were lyzed in RIPA buffer. TRAP activity was determined by a PNPP assay as described in Materials and Methods. $^{*}P < 0.05$. **B**: TRAP stained osteoclasts transfected with Nox4 and p22. **C**: TRAP stained osteoclasts transfected with a control DNA. [Color figure can be viewed in the online issue, which is available at www.interscience.wiley.com.]

activity. The decrease of cathepsin K and TRAP mRNA expression by R-Nox4 supports our previous findings that the Nox4 antisense oligonucleotide reduced osteoclastic superoxide production and bone resorption [Yang et al., 2001].

Effect of Transfection on the Signal Transduction Pathway

To determine if DNA transfection could affect the NF-κB signal transduction pathway, nuclear proteins were extracted from RAW-derived osteoclasts transfected with Nox4, Nox4/P22, and a control vector. The DNA binding activity of NF-κB was examined. As shown in Figure 4, the binding activity of NF-κB was inhibited in osteoclasts transfected with Nox4/P22. Such inhibition seems related to the level of superoxide production in transfected cells; the higher the amount of superoxide generated by Nox4/P22 transfected cells, the greater the inhibition. When EMSA was performed in the presence of

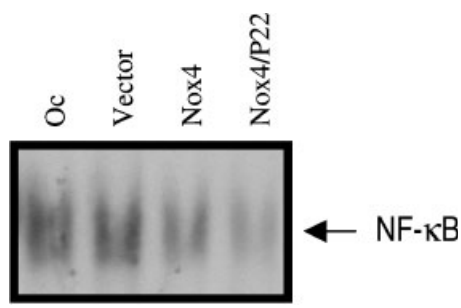

Fig. 4. The NF-κB binding activity in transfected osteoclasts. RAW-derived osteoclasts were transfected with a control vector, Nox4, and Nox4/P22 DNAs, respectively. After culturing for 24 h, nuclear protein was extracted and 20 μg of nuclear protein was incubated with the ^{32}P-labeled NF-κB consensus sequence. The protein binding activity to the NF-κB consensus sequence was visualized by autoradiography. Transfection with Nox4/P22 DNA resulted in a decrease of the NF-κB binding activity. The shown figure represents one of two repeat experiments. Oc, osteoclasts.

excess unlabeled NF-κB oliogonucleotide, no binding activity was detected (data not shown). This result indicates the specificity of the NF-κB binding.

The JNK pathway was further examined. Figure 5 showed that Nox4/p22 transfection induced JNK activity in osteoclasts, and the increase in JNK activity may relate to the increased amount of superoxide in transfected cells.

DISCUSSION

Osteoclast-generated superoxide is necessary for bone resorption to occur optimally, and this superoxide directly participates in bone degradation. Studies have shown that superoxide production occurs at the osteoclast–bone interface [Key et al., 1990; Darden et al., 1996]. Inhibition of superoxide production at the osteoclast–bone interface is associated with a reduction in bone resorption by individual osteoclasts [Ries et al., 1992]. Osteocalcin can be fragmented into small peptides upon exposure to superoxide [Key et al., 1994]. Studies have shown that NADPH oxidase is the enzyme responsible for superoxide generation in osteoclasts [Steinbeck et al., 1994; Yang et al., 1998] and p91 is the rate-limit subunit of NADPH oxidase.

We found that osteoclasts of p91 knockout mice produce normal amounts of superoxide. In keeping with this observation, similar findings have been reported that lung endothelial cells [Kubo et al., 1996] and vascular cells [Souza et al., 2002] from p91(−/−) mice are capable of generating a normal level of superoxide. This unexpected result led us to clone mouse Nox4 [Yang et al., 2001], one of the Nox family members [Lambeth et al., 2000]. Murine osteoclasts were shown to express Nox4, and the antisense oligonucleotide of Nox4 reduced superoxide generation and inhibited bone resorption in p91 knockout mice [Yang et al., 2001].

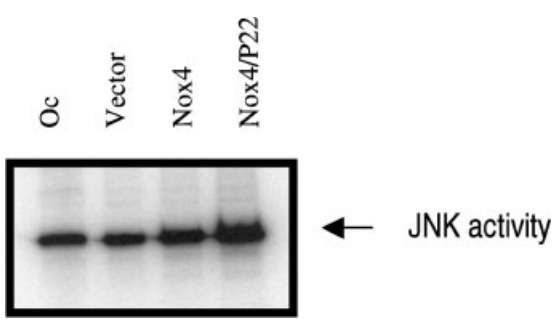

Fig. 5. The JNK kinase activity in transfected RAW derived osteoclasts. RAW-derived osteoclasts were transfected with a control vector, Nox4, and Nox4/P22 DNAs, respectively. After culturing for 24 h, total protein lysate was prepared using the lysis buffer. Immunoprecipitation was conducted with the JNK antibody (2 μg) and the protein A/G agarose. The kinase activity of the precipitated JNK was determined by the phosphorylation of the recombinant c-jun protein. An increase of JNK activity was observed in Nox4/P22 transfected osteoclasts. Shown here is one of two repeat experiments. Oc, osteoclasts.

In this study, we showed that Nox4 expression was localized in osteoclasts in situ (Fig. 1A,B). As osteoclasts developed and formed, Nox4 expression increased compared with that of precursor cells (Fig. 1C), suggesting that Nox4 may be associated with osteoclast development and formation.

Since superoxide production by osteoclasts has been linked with osteoclastic activity, a gain of function study, using the DNA transfection technique, was applied to establish an active osteoclast model. This cell model has the potential to produce a relatively high level of superoxide and/or its related ROS, which may be involved in osteoclastic function and activity.

The high expression of Nox4 mRNA in transfected osteoclasts was demonstrated (Table II), indicating the success of transfection. However, superoxide production was only enhanced slightly in those Nox4 transfected osteoclasts (Fig. 2A). Considering the fact that p91 usually combines with P22 to function as a cell membrane cytochrome b_{558} to produce superoxide [Segal, 1993], Nox4 may need the p22 subunit to form a functional complex in RAW derived osteoclasts. Therefore, cotransfection of osteoclasts with Nox4 and P22 was conducted. As expected, superoxide production was increased greatly in osteoclasts cotransfected with Nox4 and P22.

Published papers described Nox4 transfection into cell lines NIH/3T3 cells [Geiszt et al., 2000] and COS7 cells [Shiose et al., 2001], respectively. Their data showed that Nox4 transfected cells were active in the absence of p22. Both NIH/3T3 cells and COS7 cells are fibroblasts, which may contain different cellular proteins and components from osteoclasts. Therefore, Nox4 may not need an accessory protein for producing superoxide in fibroblasts. It is also possible that fibroblasts may express unknown p22 homolog, which functions as p22 to bind with Nox4 to produce superoxide. In our study, osteoclasts are the target cells for Nox4 transfection, which might contain different

biochemical and physiological proteins from fibroblasts (NIH/3T3 and COS7). Thus, p22 may be needed for osteoclasts to produce a large amount of superoxide. Another possible effect of p22 in osteoclasts is a binding with Nox4, forming a heterodimer, thus stabilizing Nox4.

Cotransfection of Nox4 and P22 increased both cathepsin K and TRAP expression in RAW derived osteoclasts (Table III). Further study showed that enhanced TRAP activity was found in osteoclasts transfected with Nox4 and P22 (Fig. 3). Such an increase may be related to an increase of superoxide production, because increased levels of cathepsin K and TRAP were diminished in cells transfected with R-Nox4/P22, which were incapable of stimulating superoxide production. Enhanced gene expression of cathepsin K and TRAP might indicate a higher potential of osteoclastic activity, since cathepsin K is directly produced by osteoclasts in order to digest demineralized bone matrix proteins [Inui et al., 1997]. TRAP is believed to be a histological marker of osteoclasts [Minkin, 1982]. More importantly, TRAP was reported to be able to generate ROS, including superoxide [Halleen et al., 1999]. In resorbing osteoclasts, TRAP facilitates breaking down matrix components in transcytotic compartments by generation of ROS [Halleen et al., 1999].

In biological systems, the generation of superoxide is accompanied by the production of hydrogen peroxide via dismutation. It has been reported that hydrogen peroxide, originated from superoxide, is the relevant molecule that activates mitogenic signal pathways, mediates cell differentiation and growth in NIH 3T3 cells [Arnold et al., 2001]. In osteoclasts, both superoxide and hydrogen peroxide have been found to play a role. Hydrogen peroxide may stimulate bone resorption by enhancing the differentiation and formation of mature osteoclasts [Fujimiya et al., 1997; Steinbeck et al., 1998]. Superoxide may stimulate bone resorption by activating collagenases [Weiss et al., 1985] and by participating in fragmentation of matrix proteins [Key et al., 1994]. In addition, superoxide may function as an antagonist to osteoclastic nitric oxide, which is a powerful inhibitor of osteoclastic bone resorption [Silverton et al., 1999].

In this study, we showed that the activation of NF-κB was inhibited rather than stimulated in Nox4/p22 transfected osteoclasts, and the JNK activity was increased by the Nox4/p22 transfection. Although we do not have direct evidence demonstrating that superoxide or its relevant ROS functions as intracellular messengers in osteoclasts, a number of reports have suggested that one of the physiological functions of superoxide and/or ROS is to regulate signaling pathways, such as modulation of rate and extent of protein phosphorylation [Fialkow et al., 1993; Chanock et al., 1994; Brumell et al., 1996; Suzuki et al., 1997; Rhee et al., 2000; Ullrich and Bachschmid, 2000]. Protein tyrosine phosphatases (PTPs) have been regarded as targets of ROS. One of PTPs family members, PP2B (also known as calcineurin), can be inactivated by superoxide as a result of oxidative damage to the Fe–Zn active center of PP2B [Wang et al., 1996]. Inhibition of other PTPs by hydrogen peroxide has also reported [Cunnick et al., 1998; Lee and Esselman, 2002; Chiarugi et al., 2003]. In addition, ROS has been shown to activate protein kinases, such as MAPK [Cunnick et al., 1998; Lee and Esselman, 2002] and JNK [Pani et al., 2000]. Because the extent of protein phosphorylation in a cell is controlled by a balance between protein kinases and phosphatases, either activation of kinases or inhibition of phosphatases would result in an elevated level of protein phosphorylation in a cell. Thus enhanced protein phosphorylation in osteoclasts may be one of the mechanisms to explain induced JNK activity in Nox4/P22 transfected osteoclasts, since protein phosphorylation has been reported to be necessary for JNK activation [Barrett et al., 1999].

Superoxide derived molecules (hydrogen peroxide, peroxynitrite, and hypochloric acid) are highly reactive and powerful oxidizers [Silverton, 1994]. It has reported that activation of NF-κB was inhibited by cell pretreatment with hydrogen peroxide [Carballo et al., 1999]. This inactivation was interpreted as resulting from oxidative damage of NF-κB. This mechanism is in agreement with the report that activity of NF-κB was totally abolished when oxidation of NF-κB occurred [Okamoto et al., 2002]. Our result may be an additional example to support the finding that inhibition of NF-κB may have resulted from oxidative damage by superoxide and superoxide derived molecules.

In summary, we demonstrated that Nox4 was expressed by osteoclasts, and Nox4 was upregulated during RANKL-mediated osteoclast development from precursor cells. Expression of Nox4 increases superoxide generation in

parallel, with increasing expression of Cathepsin K and TRAP in osteoclasts transfected by Nox4/P22. Activation of JNK and inhibition of NF-κB were also found in osteoclasts transfected by Nox4/P22. These findings suggest that superoxide and/or superoxide derived molecules may modulate the signal transduction pathways necessary for osteoclasts to function.

ACKNOWLEDGMENTS

The authors thank Amgen, Inc. for providing RANKL, and thank Mary Jacobs for critical reading.

REFERENCES

Andrews NC, Faller DV. 1991. A rapid micropreparation technique for extraction of DNA-binding proteins from limiting numbers of mammalian cells. Nucleic Acids Res 19(9):2499.

Arnold RS, Shi J, Murad E, Whalen AM, Sun CQ, Polavarapu R, Parthasarathy S, Petros JA, Lambeth JD. 2001. Hydrogen peroxide mediates the cell growth and transformation caused by the mitogenic oxidase Nox1. Proc Natl Acad Sci USA 98(10):5550–5555.

Barrett WC, DeGnore JP, Keng YF, Zhang ZY, Yim MB, Chock PB. 1999. Roles of superoxide radical anion in signal transduction mediated by reversible regulation of protein-tyrosine phosphatase 1B. J Biol Chem 274(49): 34543–34546.

Berger CE, Rathod H, Gillespie JI, Horrocks BR, Datta HK. 2001. Scanning electrochemical microscopy at the surface of bone-resorbing osteoclasts: Evidence for steady-state disposal and intracellular functional compartmentalization of calcium. J Bone Miner Res 16(11):2092–2102.

Brumell JH, Burkhardt AL, Bolen JB, Grinstein S. 1996. Endogenous reactive oxygen intermediates activate tyrosine kinases in human neutrophils. J Biol Chem 271(3):1455–1461.

Carballo M, Marquez G, Conde M, Martin-Nieto J, Monteseirin J, Conde J, Pintado E, Sobrino F. 1999. Characterization of calcineurin in human neutrophils. Inhibitory effect of hydrogen peroxide on its enzyme activity and on NF-kappaB DNA binding. J Biol Chem 274(1):93–100.

Chanock SJ, Benna J, Smith RM, Babior BM. 1994. The respiratory burst oxidase. J Biol Chem 269:24519–24522.

Chiarugi P, Pani G, Giannoni E, Taddei L, Colavitti R, Raugei G, Symons M, Borrello S, Galeotti T, Ramponi G. 2003. Reactive oxygen species as essential mediators of cell adhesion: The oxidative inhibition of a FAK tyrosine phosphatase is required for cell adhesion. J Cell Biol 161(5):933–944.

Cunnick JM, Dorsey JF, Mei L, Wu J. 1998. Reversible regulation of SHP-1 tyrosine phosphatase activity by oxidation. Biochem Mol Biol Int 45(5):887–894.

Darden AG, Ries WL, Wolf WC, Rodriguiz RM, Key LL, Jr. 1996. Osteoclastic superoxide production and bone resorption: Stimulation and inhibition by modulators of NADPH oxidase. J Bone Miner Res 11(5):671–675.

Fialkow L, Chan CK, Grinstein S, Downey GP. 1993. Regulation of tyrosine phosphorylation in neutrophils by the NADPH oxidase. Role of reactive oxygen intermediates. J Biol Chem 268(23):17131–17137.

Fujimiya K, Sugihara K, Nishikawa T. 1997. Experimental study on the role of osteoclasts and free radicals in the mandibular invasion of VX2 carcinoma in Japanese white rabbits. Bone 20(3):245–250.

Garrett IR, Boyce BF, Oreffo RO, Bonewald L, Poser J, Mundy GR. 1990. Oxygen-derived free radicals stimulate osteoclastic bone resorption in rodent bone in vitro and in vivo. J Clin Invest 85(3):632–639.

Geiszt M, Kopp JB, Varnai P, Leto TL. 2000. Identification of renox: An NAD(P)H oxidase in kidney. Proc Natl Acad Sci USA 97(14):8010–8014.

Hall TJ, Schaeublin M, Jeker H, Fuller K, Chambers TJ. 1995. The role of reactive oxygen intermediates in osteoclastic bone resorption. Biochem Biophys Res Commun 207(1):280–287.

Halleen JM, Raisanen S, Salo JJ, Reddy SV, Roodman GD, Hentunen TA, Lehenkari PP, Kaija H, Vihko P, Vaananen HK. 1999. Intracellular fragmentation of bone resorption products by reactive oxygen species generated by osteoclastic tartrate-resistant acid phosphatase. J Biol Chem 274(33):22907–22910.

Hsu H, Lacey DL, Dunstan CR, Solovyev I, Colombero A, Timms E, Tan HL, Elliott G, Kelley MJ, Sarosi I, Wang L, Xia XZ, Elliott R, Chiu L, Black T, Scully S, Capparelli C, Morony S, Shimamoto G, Bass MB, Boyle WJ. 1999. Tumor necrosis factor receptor family member RANK mediates osteoclast differentiation and activation induced by osteoprotegerin ligand. Proc Natl Acad Sci USA 96(7):3540–3545.

Inui T, Ishibashi O, Inaoka T, Origane Y, Kumegawa M, Kokubo T, Yamamura T, Cathepsin K. 1997. Antisense oligodeoxynucleotide inhibits osteoclastic bone resorption. J Biol Chem 272(13):8109–8112.

Key LL, Jr., Ries WL, Taylor RG, Hays BD, Pitzer BL. 1990. Oxygen derived free radicals in osteoclasts: The specificity and location of the nitroblue tetrazolium reaction. Bone 11(2):115–119.

Key LL, Jr., Wolf WC, Gundberg CM, Ries WL. 1994. Superoxide and bone resorption. Bone 15(4):431–436.

Kubo H, Morgenstern D, Quinlan WM, Ward PA, Dinauer MC, Doerschuk CM. 1996. Preservation of complement-induced lung injury in mice with deficiency of NADPH oxidase. J Clin Invest 97:2680–2684.

Lambeth JD, Cheng G, Arnold RS, Edens WA. 2000. Novel homologs of gp91phox. Trends Biochem Sci 25(10):459–461.

Lee K, Esselman WJ. 2002. Inhibition of PTPs by H(2)O(2) regulates the activation of distinct MAPK pathways. Free Radic Biol Med 33(8):1121–1132.

Minkin C. 1982. Bone acid phosphatase: Tartrate-resistant acid phosphatase as a marker of osteoclast function. Calcif Tissue Int 34(3):285–290.

Okamoto T, Asamitsu K, Tetsuka T. 2002. Thioredoxin and mechanism of inflammatory response. Methods Enzymol 347:349–360.

Pani G, Colavitti R, Borrello S, Galeotti T. 2000. Endogenous oxygen radicals modulate protein tyrosine phosphorylation and JNK-1 activation in lectin-stimulated thymocytes. Biochem J 347(Pt 1):173–181.

Rhee SG, Bae YS, Lee SR, Kwon J. 2000. Hydrogen peroxide: A key messenger that modulates protein phosphorylation through cysteine oxidation. Sci STKE 53:PE1.

Ries WL, Key LL, Jr., Rodriguiz RM. 1992. Nitroblue tetrazolium reduction and bone resorption by osteoclasts in vitro inhibited by a manganese-based superoxide dismutase mimic. J Bone Miner Res 7(8):931–939.

Segal AW. 1993. Structure of the NADPH-oxidase: Membrane components. Immunodeficiency 4(1–4):167–179.

Shiose A, Kuroda J, Tsuruya K, Hirai M, Hirakata H, Naito S, Hattori M, Sakaki Y, Sumimoto H. 2001. A novel superoxide-producing NAD(P)H oxidase in kidney. J Biol Chem 276(2):1417–1423.

Silverton S. 1994. Osteoclast radicals. J Cell Biochem 56(3):367–373.

Silverton SF, Adebanjo OA, Moonga BS, Awumey EM, Malinski T, Zaidi M. 1999. Direct microsensor measurement of nitric oxide production by the osteoclast. Biochem Biophys Res Commun 259(1):73–77.

Singh H, Sen R, Baltimore D, Sharp PA. 1986. A nuclear factor that binds to a conserved sequence motif in transcriptional control elements of immunoglobulin genes. Nature 319(6049):154–158.

Souza HP, Laurindo FR, Ziegelstein RC, Berlowitz CO, Zweier JL. 2002. Vascular NAD(P)H oxidase is distinct from the phagocytic enzyme and modulates vascular reactivity control. Am J Physiol Heart Circ Physiol 282(2):H466–H474.

Steinbeck MJ, Appel WH, Verhoeven AJ, Karnovsky MJ. 1994. NADPH-oxidase production of superoxide by osteoclasts actively resorbing bone. J Cell Biol 126:765–772.

Steinbeck MJ, Kim JK, Trudeau MJ, Hauschka PV, Karnovsky MJ. 1998. Involvement of hydrogen peroxide in the differentiation of clonal HD-11EM cells into osteoclast-like cells. J Cell Physiol 176:574–587.

Suzuki YJ, Forman HJ, Sevanian A. 1997. Oxidants as stimulators of signal transduction. Free Rad Biol Med 22(1–2):269–285.

Ullrich V, Bachschmid M. 2000. Superoxide as a messenger of endothelial function. Biochem Biophys Res Commun 278(1):1–8.

Wang X, Culotta VC, Klee CB. 1996. Superoxide dismutase protects calcineurin from inactivation. Nature 383(6599): 434–437.

Wei S, Wang MW, Teitelbaum SL, Ross FP. 2002. Interleukin-4 reversibly inhibits osteoclastogenesis via inhibition of NF-kappa B and mitogen-activated protein kinase signaling. J Biol Chem 277(8):6622–6630.

Weiss SJ, Peppin G, Ortiz X, Ragsdale C, Test ST. 1985. Oxidative autoactivation of latent collagenase by human neutrophils. Science 227(4688):747–749.

Yang S, Ries WL, Key LL. 1998. NADPH oxidase in the formation of superoxide in osteoclasts. Calcif Tissue Int 63:346–350.

Yang S, Madyastha P, Bingel S, Ries W, Key L. 2001. A new superoxide-generating oxidase in murine osteoclasts. J Biol Chem 276(8):5452–5458.